Available online at www.sciencedirect.com
ScienceDirect
Journal of Nutritional Biochemistry 21 (2010) 1178–1185
Journal of Nutritional Biochemistry

Abscisic acid ameliorates atherosclerosis by suppressing macrophage and CD4$^+$ T cell recruitment into the aortic wall☆

Amir J. Guri[a], Sarah A. Misyak[a], Raquel Hontecillas[a], Alyssa Hasty[b], Dongmin Liu[a], Hongwei Si[a], Josep Bassaganya-Riera[a,*]

[a]Nutritional Immunology and Molecular Nutrition Laboratory, Virginia Bioinformatics Institute, Virginia Polytechnic Institute and State University, Blacksburg, VA 24061, USA
[b]Vanderbilt University School of Medicine, Nashville, TN 37232, USA

Received 30 June 2009; received in revised form 23 September 2009; accepted 5 October 2009

Abstract

Abscisic acid (ABA) is a natural phytohormone which improves insulin sensitivity and reduces adipose tissue inflammation when supplemented into diets of obese mice. The objective of this study was to investigate the mechanisms by which ABA prevents or ameliorates atherosclerosis. apolipoprotein E-deficient (ApoE$^{-/-}$) mice were fed high-fat diets with or without ABA for 84 days. Systolic blood pressure was assessed on Days 0, 28, 56 and 72. Gene expression, immune cell infiltration and histological lesions were evaluated in the aortic root wall. Human aortic endothelial cells were used to examine the effect of ABA on 3′,5′-cyclic adenosine monophosphate (cAMP) and nitric oxide (NO) production in vitro. We report that ABA-treated mice had significantly improved systolic blood pressure and decreased accumulation of F4/80$^+$CD11b$^+$ macrophages and CD4$^+$ T cells in aortic root walls. At the molecular level, ABA significantly enhanced aortic endothelial nitric oxide synthase (eNOS) and tended to suppress aortic vascular cell adhesion molecule-1 (VCAM-1) and monocyte chemoattractant protein-1 (MCP-1) expression and plasma MCP-1 concentrations. ABA also caused a dose-dependent increase in intracellular concentrations of cAMP and NO and up-regulated eNOS mRNA expression in human aortic endothelial cells. This is the first report showing that ABA prevents or ameliorates atherosclerosis-induced hypertension, immune cell recruitment into the aortic root wall and up-regulates aortic eNOS expression in ApoE$^{-/-}$ mice.

Keywords: ABA; eNOS; cAMP; Atherosclerosis; ApoE$^{-/-}$ mice; Inflammation; Aorta

1. Introduction

The isoprenoid phytohormone abscisic acid (ABA), one of the five major classes of plant hormones, plays important roles during seed development and dormancy, in plant responses to various environmental stresses and host response. ABA improves glucose tolerance and decreases macrophage accumulation in white adipose tissue of obese, diabetic mice [1,2]. The effect of ABA on adipose tissue macrophage accumulation was shown to be partially dependent on the presence of peroxisome proliferator-activated receptor γ (PPAR γ) in immune cells [3]. Because cardiovascular disease (CVD) is the number one killer of adults in the United States [4], given that macrophages and foam cells play a crucial role in atherosclerotic plaque formation, and based on the fact that ABA suppresses macrophage accumulation in tissues and modulates immune responses, the purpose of this study is to assess whether ABA is effective in preventing or ameliorating atherosclerosis in mice and to elucidate ABA's cellular and molecular mechanisms of action in the vascular wall.

Bruzzone et al. demonstrated that ABA stimulates insulin release from pancreatic islets via 3′,5′-cyclic adenosine monophosphate (cAMP) signaling [5]. cAMP controls heart rate and muscle contraction [6]. In addition, it regulates the passage of calcium through ion channels in the cell membrane [6]. Glucagon-like peptide 1 receptor agonists represent another example of cardioprotective and antidiabetic agents that signal through cAMP [7]. More specifically, ligand binding to stimulatory and inhibitory G protein-coupled receptors regulates the cAMP-synthesizing activity of adenylate cyclase [8]. Increased cAMP signaling ameliorates hypertension in rats, in part through increasing the expression of endothelial nitric oxide synthase (eNOS) [9,10]. Thus, it is possible that ABA-induced vascular relaxation is mediated in part through cAMP-dependent mechanisms. Furthermore, elevated cAMP has been shown to ameliorate ischemia-reperfusion injury in rat cardiac allografts by decreasing vascular cell adhesion molecule-1 (VCAM-1) expression- a protein involved in the transmigration of macrophages and T cells into vascular lesions [11]. Based on this background, we hypothesized that ABA may exert its vasoprotective effects through a cAMP-dependent mechanism via suppressing macrophage and T cell recruitment into the aortic root wall.

We demonstrate for the first time that ABA decreases atherosclerosis-related hypertension in apolipoprotein E-deficient (ApoE$^{-/-}$)

☆ Disclosures: none.
* Corresponding author. Tel.: +1 540 231 7421; fax: +1 540 231 2606.
E-mail address: jbassaga@vt.edu (J. Bassaganya-Riera).

0955-2863/$ - see front matter © 2010 Elsevier Inc. All rights reserved.
doi:10.1016/j.jnutbio.2009.10.003

mice, a preventive effect we propose is mediated by decreased expression of MCP-1 and vascular cell adhesion molecule-1 (VCAM-1), suppressed macrophage and T cell infiltration into the wall of the aortic root, and up-regulation of endothelial nitric oxide synthase (eNOS). In addition to showing that ABA causes changes in gene expression and immune cell infiltration, we demonstrate that at nanomolar concentrations, ABA augments endothelial cell cAMP and nitric oxide (NO) concentrations in a dose-dependent manner and increases eNOS expression, suggesting that cAMP and eNOS are putative molecular targets in endothelial cells.

2. Materials and methods

2.1. Animal procedures

Five-week old ApoE$^{-/-}$ mice (n=40) were housed at the animal facilities at Virginia Polytechnic Institute and State University in a room maintained at 75°F, with a 12:12-h light–dark cycle starting from 6 a.m. All experimental procedures were approved by the Institutional Animal Care and Use Committee of Virginia Polytechnic Institute and State University and met or exceeded requirements of the Public Health Service/National Institutes of Health and the Animal Welfare Act. Mice were fed a high saturated fat (AIN-93G-based) diet containing 19.6% fat and 0.2% total cholesterol and obtaining 40.1% of kcal from fat (4.4 kcal/g) with or without 100 mg/kg of a racemic ABA mixture [3]. Systolic blood pressure was assessed on Days 0, 28, 56 and 72. On Day 84, fasted mice (12 h) were sacrificed by carbon dioxide asphyxiation and blood was withdrawn through cardiac puncture. Glucose concentrations of whole blood were assessed with an Accu-Chek Glucometer (Roche, Indianapolis, IN, USA), and plasma insulin was measured through insulin enzyme-linked immunosorbent assay (ELISA) (Millipore, Billerica, MA, USA). Aortas were collected for analysis of immune cell infiltration, histological evaluation of atherosclerotic lesions and gene expression analyses.

2.2. Blood pressure assessment

Systolic blood pressure was measured with a computerized noninvasive tail-cuff system (CODA 2 mouse rat blood pressure system; Kent Scientific, Torrington, CT, USA). Conscious animals were kept in a restrainer, with a standard acclimatization time of 10 min and gentle heating of the tail before every recording session. Fifteen recordings, which were preceded by five acclimitization recordings, were performed on each animal during each timepoint.

2.3. Plasma lipid and fast performance liquid chromatography analysis

Plasma cholesterol and triglyceride (TG) levels were measured using kits from Raichem (San Diego, CA, USA) adapted for microtiter plate assays. Plasma free fatty acids were measured using the Non-esterified fatty acids (NEFA)-HR(2) kit from Wako. Fast performance liquid chromatography (FPLC) separation of plasma lipoproteins was performed on a Superose 6 column using buffer containing 0.15 M NaCl, 0.01 M Na_2HPO_4 and 1 mM EDTA at a flow rate of 0.5 ml/min. Forty 0.5-ml fractions were collected and cholesterol was measured in fractions 10–40. Fractions 15–20 contain very low-density lipoprotein (VLDL), fractions 21–27 contain low-density lipoprotein (LDL), and fractions 28–34 contain high-density lipoprotein (HDL).

2.4. Digestion of aorta

After euthanization, mouse hearts were perfused with phosphate-buffered saline (PBS) for 2 min. Aortas were then extracted. Aortic roots were cut into small >1-mm^3 pieces, and placed in 1× Hanks Balanced Sodium Salt Solution (HBSS) containing 0.2% type II collagenase (Worthington Biochemicals). After digestion at 37°C for 1 h, samples were sent through a 100-mm nylon filter (BD), washed with HBSS and centrifuged at 1200 rpm for 10 min. Cell suspensions were then resuspended in flow cytometry associated cell sorting (FACS) buffer and enumerated by using a Z1 Single-Particle Counter (Beckman Coulter).

2.5. Flow cytometry

Aortic root wall-derived cells (i.e., tunica intima, media and adventitia) were seeded into 96-well plates and centrifuged at 4°C at 3000 rpm for 4 min. To assess differential monocyte/macrophage infiltration, the cells were then incubated in the dark at 4°C for 20 min in FcBlock (20 μg/ml; BD Pharmingen) for macrophage assessment, and then for an additional 20 min with fluorochrome-conjugated primary antibodies anti-F4/80-PE-Cy5 (5 μg/ml, eBioscience) and anti-CD11b-FITC (2 μg/ml, eBioscience). For lymphocyte assessment, cells were incubated with CD4-FITC (2 μg/ml; BD Pharmingen) and CD3 PE-Cy5 (2 μg/ml; BD Pharmingen). After incubation with primary antibodies, cells were centrifuged at 4°C at 3000 rpm for 4 min and washed with 200 μl of FACS buffer. After washing, cells were suspended in 200 μl PBS and 3-color data acquisition was performed on a FACS Calibur flow cytometer. Data analyses were performed by using the CellQuest software (BD).

2.6. Histology analyses of the aorta

The aortic root sections used for histological analyses were perfusion-fixed with paraformaldehyde. Samples of aorta were cut transversally, stained with hematoxylin and eosin and analyzed histologically. Areas for the lumen, tunica media and aortic lesions and the thicknesses of the tunica intima and media were assessed using Image Pro Plus 6.1 software (Media Cybernetics, Bethesda, MD, USA). For thickness analyses, eight different measurements from the intima and media were taken using previously described methods [12]. For semiquantitative assessment of lesion severity, methods described by van Vlijmen et al were used [13]. Briefly, lesions were classified into five categories (1) early fatty streak: per section up to 10 foam cells present in the intima; (2) regular fatty streak: more than 10 cells present in the intima; (3) mild plaque: extension of foam cells into the media and mild fibrosis of the media without significant loss in architecture; (4) moderate plaque: foam cells in media, fibrosis, cholesterol clefts, mineralization and/or necrosis of the media and (5) severe plaque: as 4 but more extensive and deeper in the media. Scoring classifications were applied to 15 lesions from control and ABA-fed mice. Lesions falling in categories 1–3 were classified as mild and 4–5 as severe.

2.7. Quantitative real-time reverse transcriptase-polymerase chain reaction

Total RNA was isolated from aorta using the RNA isolation Minikit (Qiagen) according to the manufacturer's instructions. Total RNA (1 μg) was used to generate complementary DNA (cDNA) template using the iScript cDNA Synthesis Kit (Bio-Rad, Hercules, CA, USA). The total reaction volume was 20 μl with the reaction incubated as follows in an MJ MiniCycler: 5 min at 25°C, 30 min at 52°, 5 min at 85°C and hold at 4°C. Polymerase chain reaction (PCR) was performed on the cDNA using Taq DNA polymerase (Invitrogen, Carlsbad, CA) and using previously described conditions [14]. Each gene amplicon was purified with the MiniElute PCR Purification Kit (Qiagen) and quantitated on an agarose gel by using a DNA mass ladder (Promega). These purified amplicons were used to optimize real-time PCR conditions and to generate standard curves in the real-time PCR assay. Primer concentrations and annealing temperatures were optimized for the iCycler iQ system (Bio-Rad) for each set of primers using the system's gradient protocol. PCR efficiencies were maintained between 92% and 105% and correlation coefficients above 0.98 for each primer set during optimization and also during the real-time PCR of sample DNA.

cDNA concentrations for genes of interest were examined by real-time quantitative PCR using an iCycler IQ System and the iQ SYBR green supermix (Bio-Rad). A standard curve was generated for each gene using 10-fold dilutions of purified amplicons starting at 5 pg of cDNA and used later to calculate the starting amount of target cDNA in the unknown samples. SYBR green I is a general double-stranded DNA intercalating dye and may therefore detect nonspecific products and primer/dimers in addition to the amplicon of interest. In order to determine the number of products synthesized during the real-time PCR, a melting curve analysis was performed on each product. Real-time PCR was used to measure the starting amount of nucleic acid of each unknown sample of cDNA on the same 96-well plate. Results are presented as starting quantity of target cDNA (picograms) per microgram

Table 1
Oligonucleotide sequences for quantitative real-time PCR

Primer	Sequence	Length (bp)	Accession number
β-Actin F	5′-CCCAGGCATTGCTGACAGG-3′	141	X03672
β-Actin R	5′-TGGAAGGTGGACAGTGAGGC-3′		
eNOS F	5′-CCCGGGACTTCATCAATCAGT-3′	121	NM_008713
eNOS R	5′-TCCCGGAGCTGGTAGGTG-3′		
E-selectin F	5′-CAGCTTTGCATGATGGCGTCT-3′	83	NM_011345
E-selectin R	5′-GAAGGGTACAGGCGAGTTGG-3′		
15-LOX F	5′-GCGCAGCACTCTTCCATCC-3′	106	NM_009660
15-LOX R	5′-TCGTCGCGTCCTTGGTTTTA-3′		
MCP-1 F	5′-CTTGCCTAATCCACAGACTG-3′	146	AJ238892
MCP-1 R	5′-GCCTGAACAGCACCACTA-3′		
VCAM-1 F	5′-TCTCCCAGGAATACAACGAT-3′	75	NM_011693
VCAM-1 R	5′-ACAGGTCATTGTCACAGCAC-3′		
PPAR γ F	5′CAGGCTTGCTGAACGTGAAG3′	117	NM_011146
PPAR γ R	5′GGAGCACCTTGGCGAACA3′		
CD36 F	5′CCGGGCCACGTAGAAAACA3′	156	NM_007643
CD36 R	5′CCTCCAAACACAGCCAGGAC3′		

F, forward; R, reverse. PCR primer pairs were designed for an optimal annealing temperature of 57°C and product lengths between 75 and 150 base pairs.
When plotting threshold cycle versus log starting quantity (pg), standard curves had slopes between −3.1 and −3.7; PCR efficiencies between 92 and 105 and R^2 above 0.98.

of total RNA. Primer sequences, the length of the PCR product and gene accession numbers are outlined in Table 1.

2.8. Determination of MCP-1 concentrations in plasma

A Ready-set-go MCP-1 ELISA (eBioscience) was used to quantify plasma MCP-1 according to the manufacturer's instructions.

2.9. Intracellular cAMP and NO concentrations and eNOS mRNA in human aorta endothelial cells

Confluent human aorta endothelial cells (HAECs) at passage 3 maintained with EGM-2 media (Clonetics, Walkerville, MD, USA) were adapted to Hank's buffered salt solution buffer for 30 min and then stimulated with ABA or forskolin (1 μM) for 10 min. For intracellular assessment of cAMP, the cells were harvested into 0.1 M HCl and the lysates were obtained by sonication and centrifugation. cAMP the lysates were determined by using an EIA kit (Assay Designs, Ann Arbor, MI, USA), and results were obtained from four independent experiments. Nitric oxide levels in the cell culture supernatants were determined with the Nitric Oxide Assay Kit according to manufacturer's instructions (Assay Designs). We also assessed whether treatment of HAECs with ABA would enhance eNOS mRNA expression. HAECs were treated with or without 10 μM ABA for 24 h and eNOS mRNA expression was measured by real-time PCR.

2.10. Statistics

Data from day 84 were analyzed as a completely randomized design. Blood pressure data were analyzed using repeated measures. To determine the statistical significance of the model, analysis of variance was performed using the general linear model procedure of SAS, and $P<.05$ was considered to be significant.

3. Results

3.1. ABA supplementation has no effect on body weight, cholesterol, glucose or insulin concentrations but increases TG and non-esterified fatty acids

ApoE$^{-/-}$ mice were fed high-fat diets with or without ABA for 84 days. Dietary ABA-supplementation had no significant effect on body weights, plasma glucose, insulin or total cholesterol levels (Table 2). ABA did significantly raise plasma TG and non-esterified fatty acid concentrations. In our FPLC analysis, we observed a slight shift in the profiles to lower VLDL and higher LDL and HDL in the ABA-fed mice, indicative of a more TG-rich VLDL (Fig. 1).

3.2. Dietary ABA supplementation improves systolic blood pressure

To determine whether ABA affects hypertension in ApoE$^{-/-}$ mice we assessed blood pressure on Days 0, 28, 56 and 72 of the dietary intervention. On Days 56 and 72, mice fed ABA had significantly reduce systolic blood pressure when compared to control-fed mice (Fig. 2). ABA had no significant affect on diastolic blood pressure or mean heart rate (data not shown).

Table 2
Effect of ABA supplementation on metabolic parameters

	Diet	
	Control	ABA
Body weight (g)	29.7±0.63	30.8±0.63
Glucose (mg/dl)	195.1±11.9	194.6±11.9
Insulin (ng/ml)	0.413±0.05	0.432±0.05
HOMA-IR	4.85±0.76	4.93±0.76
Cholesterol (mg/dl)	318.1±23.8	339.0±25.1
TGs (mg/dl)	90.5±12.3	136.1±12.3*
NEFAs (mequiv./ml)	1.51±0.17	2.05±0.17*

ApoE$^{-/-}$ mice were fed high-fat diets with or without ABA (100 mg/kg) for 84 days. Plasma from fasted mice (12 h) on day 84 were analyzed for metabolic parameters. Data are presented as least square means±S.E. Data points with an asterisk are significantly different ($P < .05$).

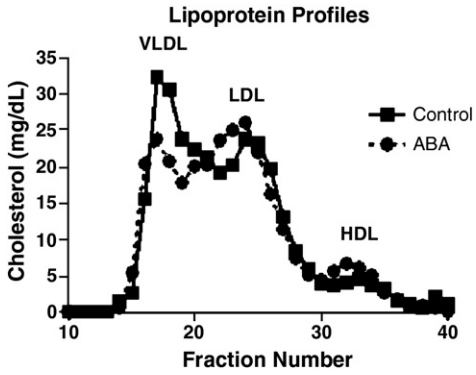

Fig. 1. FPLC separation of plasma lipoproteins was performed on a Superose 6 column using buffercontaining 0.15 M NaCl, 0.01 M Na2HPO$_4$ and 1 mM EDTA at a flow rate of 0.5 ml/min. Forty 0.5-ml fractions were collected and cholesterol was measured in fractions 10-40. Fractions 15–20 contain VLDL, fractions 21–27 contain LDL and fractions 28–34 contain HDL.

3.3. ABA decreases aortic root wall thickness, elevates aortic eNOS and 15-LOX mRNA expression and reduces atherosclerotic lesions

In line with the decrease in systolic blood pressure, there were significant histological differences in aortas of control and ABA-fed mice (Fig. 3). While there were no significant differences in luminal and media areas, aortas from ABA-supplemented mice had a significantly lower intima to media ratio (Fig. 3C-E). These differences were mainly attributable to reductions in intimal wall thickness. ABA also significantly elevated aortic expression of eNOS and 15-lipoxygenase (Fig. 3F and G), two genes involved in vasorelaxation.

To assess the affect of ABA-supplementation on atherosclerotic lesions, a semiquantitative analysis of lesion severity was performed. Fifteen lesions from control and ABA-fed mice were analyzed histologically and classified as either mild or severe using criteria described by van Vlijmen et al [13]. Eight of the 15 lesions in control-fed mice were mild and seven were severe, whereas in the ABA-fed mice 10 were mild and five were severe (Fig. 4A-C). Because atherosclerotic plaque is a significant contributor to vascular thrombosis and stenosis, we also assessed lesion areas as a percentage of lumenal area, as described by Andersson et al [15]. We found that mice fed ABA had a significantly decreased lesion area as a percentage of total lumenal area (Fig. 4D).

3.4. ABA suppresses aortic inflammation

Atherosclerosis is associated with an infiltration of macrophages and lymphocytes into the atherosclerotic plaque and a vascular

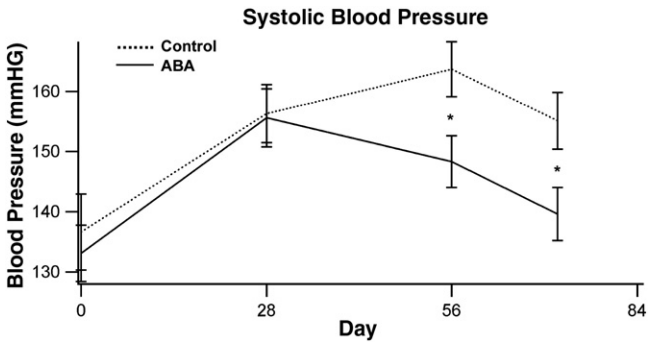

Fig. 2. ABA decreases systolic blood pressure in ApoE$^{-/-}$ mice. ApoE$^{-/-}$ mice were fed high fat diets created with (solid line) or without (dashed line) 100 mg/kg diet racemic ABA. Systolic blood pressure was assessed on Days 0, 28, 56 and 72 of dietary treatment. Data were analyzed as a completely randomized design. Data points with an asterisk are significantly different ($P < .05$).

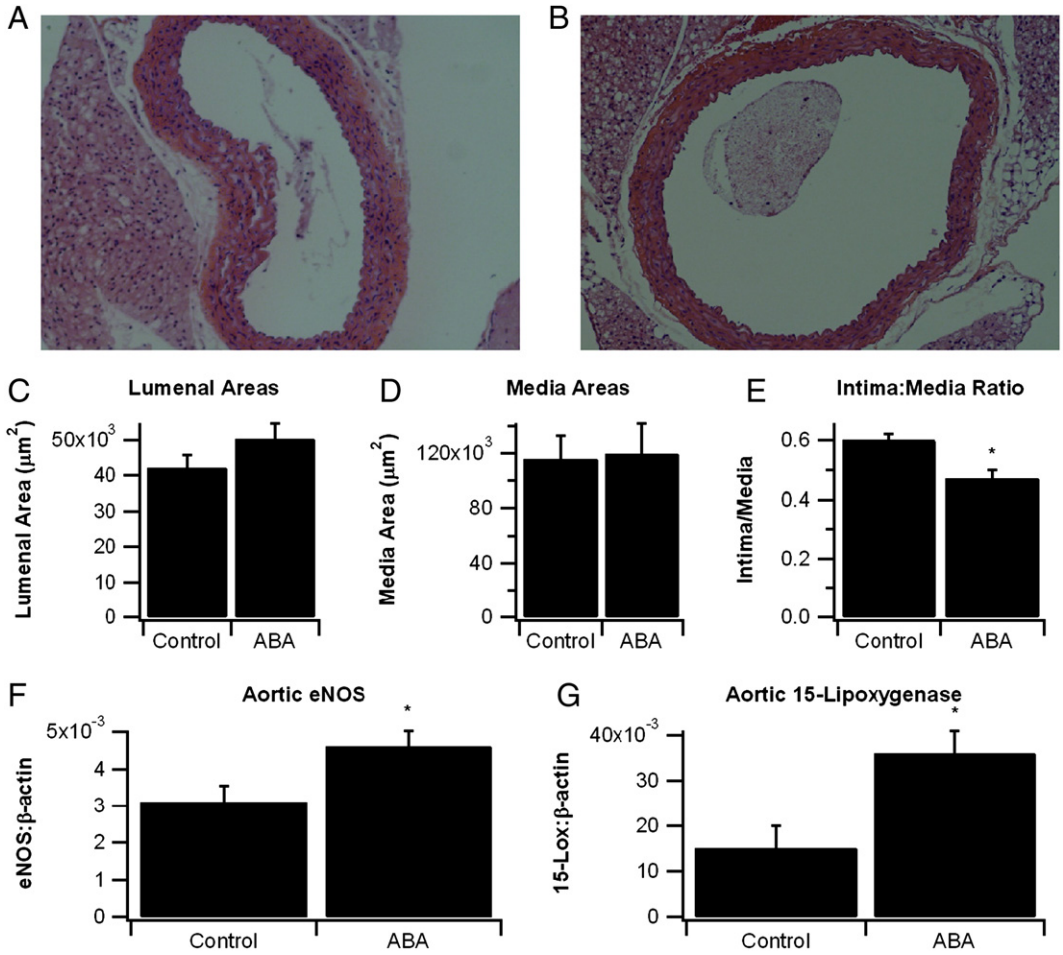

Fig. 3. Aortas were collected on Day 84 of dietary intervention. Representative photomicrographs (original magnification ×100) of aortic root specimens from (A) control and (B) ABA-fed mice. (C) Analysis of lumenal areas and (D) tunica media areas were performed with aortic cross-sections using Image Pro Plus software. (E) Aortic thickness was analyzed as a ratio of the intima to the media. Gene expression in the aorta of (F) eNOS and (G) 15-lipoxygenase (15-LOX) were measured as a ratio to the house-keeping gene β-actin. Data were analyzed as a completely randomized design. Data points with an asterisk are significantly different ($P < .05$).

remodeling of aortic wall which leads to stenosis [16,17]. Our previous findings have shown that ABA-supplementation significantly reduces macrophage infiltration into white adipose tissue and induces an approximately 15-fold reduction in MCP-1 expression in the adipose tissue stromal-vascular fraction of obese db/db mice [3]. These effects were dependent on the presence of PPAR γ in immune cells. We demonstrate here that ABA-supplementation significantly reduces recruitment of two specific immune cell populations, F4/80$^+$CD11b$^+$ macrophages and CD4$^+$ T-cells, in the aortic root (Fig. 5A). The mRNA expression of proinflammatory markers VCAM-1 (P=.07), MCP-1 (P=.10) and E-selectin (P=.20) were reduced, though not to statistical significance, in the aortic roots of ABA-fed mice, and plasma MCP-1 concentrations were decreased (P=.10, Fig. 5B-H). There were no differences in the expression of PPAR γ or its responsive genes in the aorta.

3.5. ABA increases intracellular concentration of intracellular cAMP and stimulates NO production in aortic endothelial cells

Other reports demonstrate that ABA increases intracellular levels of cAMP in pancreatic β-cells [5]. Our findings in the aorta showing increased expression of eNOS and a down-regulated trend in pro-inflammatory markers VCAM-1 and MCP-1 could be due to changes in this second messenger. To determine whether ABA increases cAMP in endothelial cells, we treated HAECs with ABA or the cAMP activator forskalin. ABA significantly increased intracellular cAMP concentrations at doses as low as 0.1 μM ABA, with 1 μM ABA inducing maximal effect (Fig. 6A). Increased cAMP concentrations correlated with enhanced NO production in ABA-treated endothelial cells (Fig. 6B). HAECs were treated with or without 10 μM ABA for 24 h, total RNA was isolated and eNOS mRNA expression was measured by real time PCR. We found that ABA significantly ($P < .02$) increased eNOS mRNA levels (Fig. 6C).

4. Discussion

CVD is the primary leading cause of death in the United States [4]. CVD is associated with atherosclerosis, the progressive build-up of plaque in the arterial walls, which, over time, can lead to occlusion of blood vessels. The objective of this study was to determine the effects of ABA on the development of atherosclerosis. To address this goal, ApoE$^{-/-}$ mice were fed either a control or ABA-supplemented high-fat, atherogenic diet for 84 days. The progression of atherosclerosis and lesion development in ApoE$^{-/-}$ mice occurs in a similar manner to that of humans. Also similar to humans, ApoE$^{-/-}$ mice undergo accelerated atherosclerosis when fed high-fat diets, with histological differences being observed as early as six weeks of age [18].

We first found differences between the groups on day 56, where we observed a significant decrease in mean systolic blood pressure in

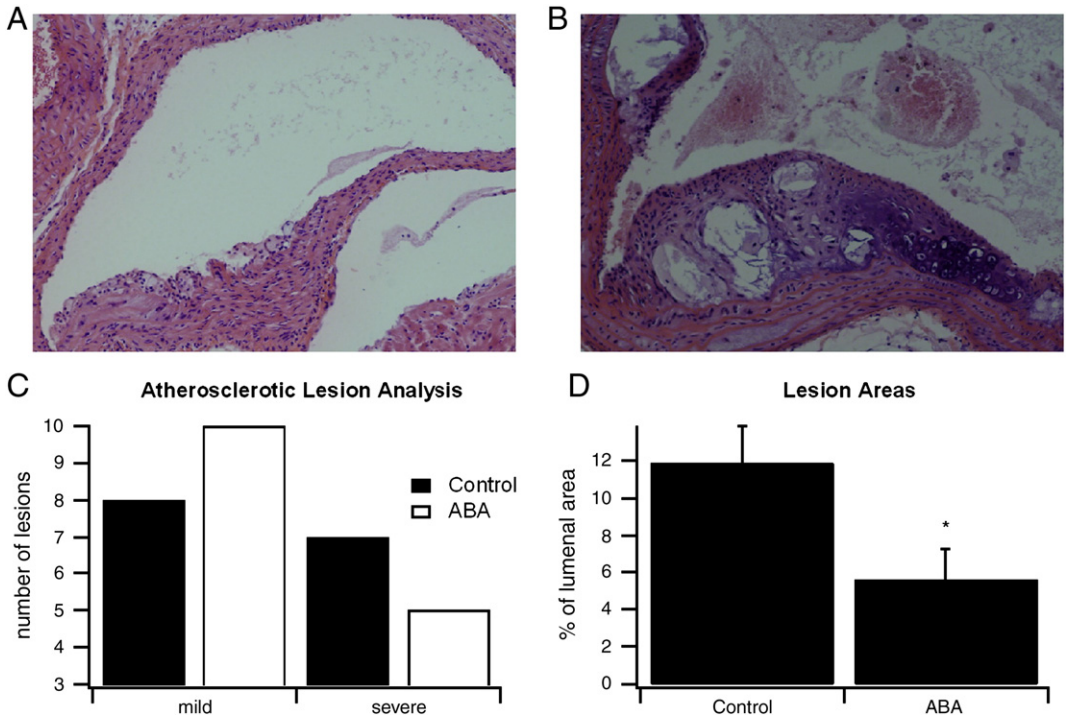

Fig. 4. Histological examination of aortic lesions. ApoE$^{-/-}$ mice were fed high fat diets created with or without ABA (100 mg/kg diet). After 84 days aortas were excised and lesions were analyzed histologically according to methods described by van Vlijmen et al[13]. Representative photomicrographs (100X) of a (A) mild and (B) severe lesion are depicted. (C) The total number of mild (categories 1-3) and severe (categories 4-5) lesions from control and ABA-fed mice are shown. (D) Lesional areas, as a percentage of total lumen area, for control and ABA-fed mice were calculated from histological sections with Image Pro Plus software. Data are represented as mean±S.E. Points with an asterisk are significantly different from the control ($P < .05$).

ABA-fed mice. This trend also continued at Day 72, in which the differences were somewhat accentuated. These in vivo findings are in line with the increased expression of eNOS and 15-LOX in aortas of ABA-fed mice and increased synthesis of nitric oxide in ABA-treated endothelial cells, though more corroborative studies are needed to validate the importance of nitric oxide and 15-LOX-metabolites to ABA's antihypertensive effects. Interestingly, 15-LOX catalizes the generation of arachidonic acid and linoleic acid-derived lipid mediators (e.g., 15-HETE and 13-HODE) which elicit anti-inflammatory and cardioprotective effects [19]. There are also studies showing that 15-LOX can exert a pro-inflammatory, atherogenic effect through increasing LDL oxidation, smooth muscle proliferation and monocyte recruitment into the vessel wall [19]. We did not observe increased aortic inflammation with the up-regulation of 15-LOX. In fact, aortic root walls from ABA-fed mice were less inflamed than those from control fed-mice. Dietary ABA-supplementation significantly reduced the percentage of F4/80^{+}CD11b^{+} macrophages and CD4^{+} lymphocytes, which are know to contribute to atherosclerotic plaque formation and obesity-related inflammation [20]. Also, mRNA for MCP-1, VCAM-1 and E-selectin and MCP-1 plasma protein levels tended to be decreased. In line with reduced inflammation, ABA-supplemented mice had fewer and less severe aortic lesions, and the area of aortic lesions was significantly reduced.

Based on a recent report by Bruzzone et al. that ABA increases cAMP in pancreatic islets [5], we assessed whether ABA induced a similar effect in endothelial cells, finding a dose-dependent relationship between ABA levels and cAMP concentration. cAMP signaling plays a major role in maintaining vascular homeostasis by inhibiting endothelial [21] and smooth muscle cell [22] proliferation, decreasing immune cell endothelial adhesion [23] and maintaining endothelial barrier function [24,25]. The expression eNOS, which we show is increased by ABA-treatment in vivo and in vitro, is also regulated in part through the cAMP response element (CRE)-responsive elements in its promoter region [26,27]. A recent study has shown that the lanthione synthetase C-like protein (LANCL2) is required for ABA binding to the membrane of human granulocytes and ABA signaling [28]. Additional loss-of-function studies are needed to determine whether ABA's effect on cAMP is LANCL2-dependent.

In our previous studies with db/db mice, ABA-supplementation improved glucose tolerance and adipose tissue inflammation through a mechanism that was partially dependent on PPAR γ [1,3], a transcription factor that inhibits nuclear factor κB (NF-κB) activation in macrophages [29]. Here, we report no significant differences in PPAR γ or its responsive genes in the aorta, a finding which of itself does not rule ABA from still activating PPAR γ in immune cells. In this case, the RNA from macrophages and T cells infiltrating the tunica intima of the aortic root may have been diluted by RNA originated from endothelial, smooth muscle cells and fibroblasts (i.e., intima, media and adventitia).

Recently, a study Magnone et al. investigated the effect of ABA on vascular smooth muscle cells and primary human monocytes in vitro, finding that ABA increases MCP-1 and MMP-9 when stimulated in culture for 6 h through Ca^{2+}/protein kinase C induced phosphorylation of NF-κB [30]. The authors concluded that ABA is proatherogenic, an interpretation which differs significantly from our in vivo findings. The report by Magnone et al demonstrates the presence of endogenous ABA in human arterial atherosclerotic plaques at a ten-fold greater concentration in comparison to uninvolved tissue [30]. While the authors of that report suggest that the presence of ABA in the plaques contributes to the pathogenesis of atherosclerosis, in light of our in vivo findings demonstrating improved intima to media ratio and decreased atherosclerotic lesions in ABA-fed mice, we suggest that the body synthesizes ABA as a part of a down-regulatory mechanism designed to dampen lesion development during atherosclerosis.

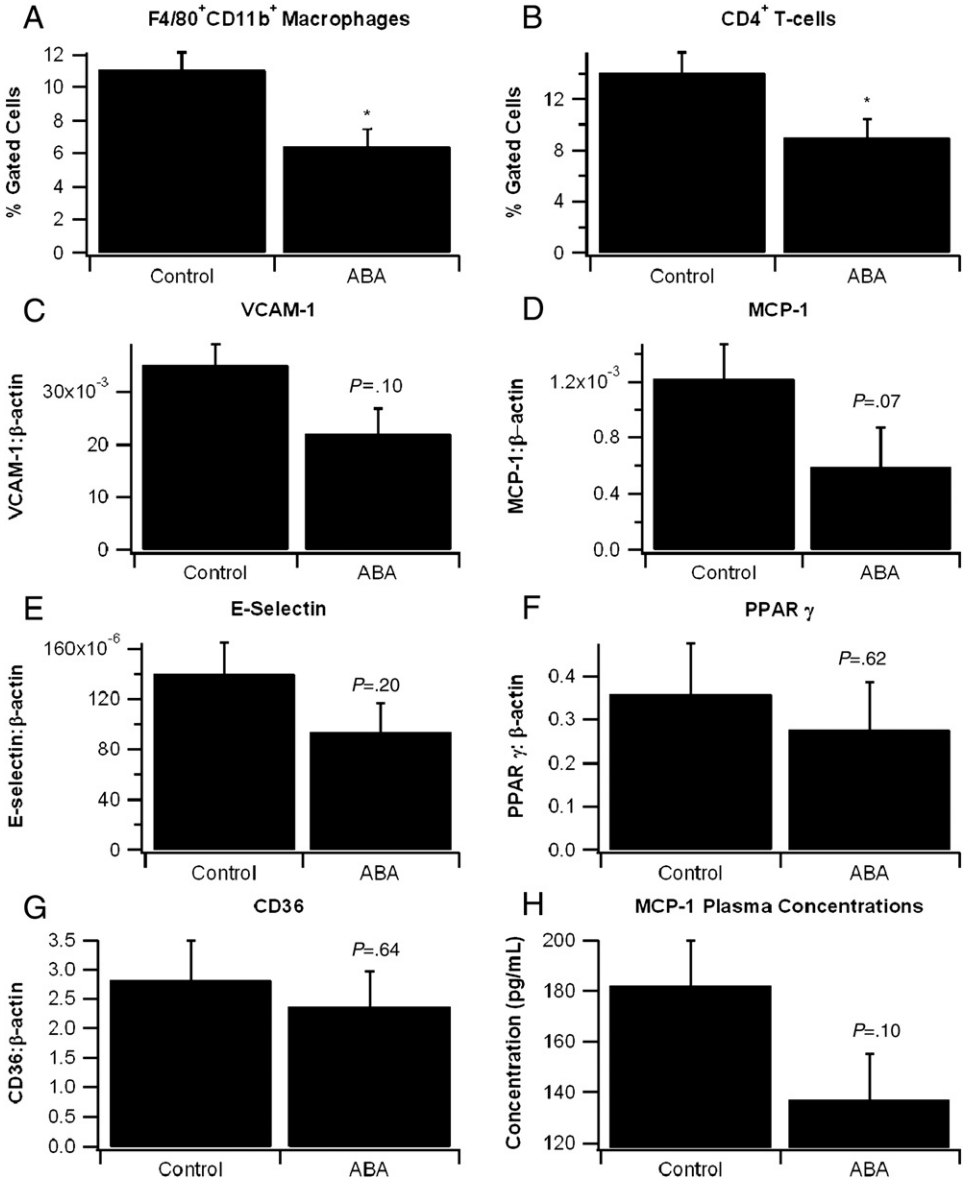

Fig. 5. ABA decreases immune cell infiltration in aortas of ApoE$^{-/-}$ mice and reduces pro-inflammatory gene expression. ApoE$^{-/-}$ mice were fed high fat diets created with or without 100 mg/kg diet racemic ABA. (A) Infiltration of F4/80^{+}CD11b^{+} macrophages and CD4^{+} T-cells into the aorta were assessed with flow cytometry. Gene expression in the aorta of pro-inflammatory markers (B) VCAM-1, (C) MCP-1, (D) E-selectin, (F) peroxisome proliferator-activated receptor γ (PPAR γ) and (G) CD36 were measured as a ratio to the housekeeping gene β-actin. (H) MCP-1 protein concentrations (pg/ml) were measured by ELISA. Data were analyzed as a completely randomized design. Data points with an asterisk are significantly different ($P < .05$).

In mouse models of overweight, obesity and diabetes, we have consistently observed that ABA supplementation ameliorates glucose tolerance, adipose tissue inflammation and liver steatosis [1,3]. In the present study, we found that ABA decreases the expression of inflammatory genes in the aorta and alleviates hypertension. This apparent paradoxical role of ABA, to increase inflammation in some conditions and lessen it in others, would be in line with ABA's role as an endogenous or dietary modulator of stress response, which is one of its many roles in plants. NEFAs, which we found were increased in plasma of ABA-fed mice, have also been described as endogenous homeostatic regulators of stress and protect endothelial cells from the cytotoxic effects of hydrogen peroxide [31]. However, the increase in plasma TG caused by ABA in this study are opposite to what we anticipated and to what our metabolic studies in db/db mice showed [3]. Our finding that ABA improves atherosclerosis despite increasing plasma TG levels and not affecting total cholesterol levels may be linked to its antihypertensive effects, as there is considerable epidemiological evidence suggesting that blood pressure effects atherosclerotic lesion development [32]. In line with these reports in humans, ApoE$^{-/-}$ mice lacking eNOS develop more severe atherosclerotic lesions [33].

In conclusion, our data indicates that ABA-supplementation elicits a local anti-atherogenic effect in the arterial wall of ApoE$^{-/-}$ mice and supports its potential as preventive and therapeutic intervention.

Acknowledgments

Supported by a grant from the National Center for Complementary and Alternative Medicine at the National Institutes of Health (5R01AT4308 to J.B.-R.), European Commission grant number

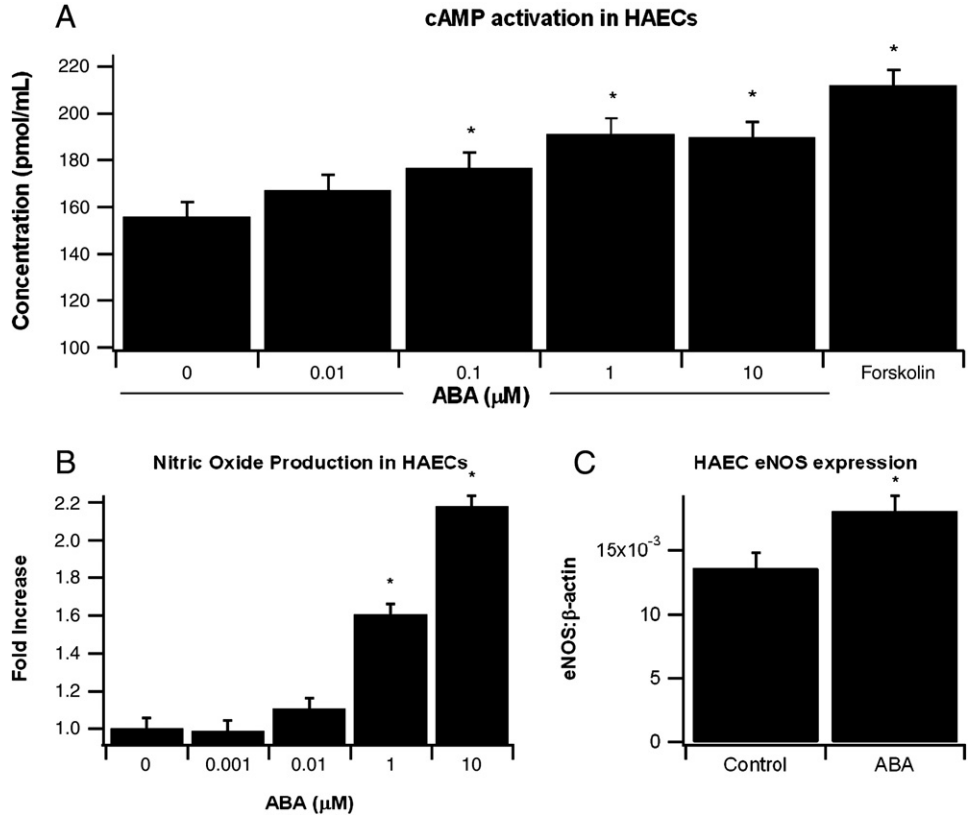

Fig. 6. (A) Confluent HAEC were serum-starved using HBSS buffer for 30 min and then stimulated with various concentrations of ABA (0, 0.01, 0.1, 1, 10 μM) or Forskolin (1 μM) for 5 min. After removing supernatant, cells were lysated with 0.1 M HCl for 20 min to measure non-acetylated cAMP. (B) Confluent HAEC were serum-starved using HBSS buffer for 30 min and then stimulated with various concentrations of ABA (0, 0.001, 0.01, 0.1, 1, 10 μM) for 15 min to measure NO. Results (pmol/ml) from four independent experiments are depicted. (C) eNOS mRNA expression after 24-h treatment with control vehicle (DMSO) or ABA (10 μM). Data are represented as mean±S.E. Points with an asterisk are significantly different from the control ($P < .05$).

224836 and funds from the Nutritional Immunology and Molecular Nutrition Laboratory.

References

[1] Guri AJ, Hontecillas R, Si H, Liu D, Bassaganya-Riera J. Dietary abscisic acid ameliorates glucose tolerance and obesity-related inflammation in db/db mice fed high-fat diets. Clin Nutr 2007;26:107–16.
[2] Bassaganya-Riera J, Skoneczka J, Kingston DGJ, et al. Mechanisms of action and medicinal applications of abscisic acid. Curr Med Chem 2009 [In press].
[3] Guri AJ, Hontecillas R, Ferrer G, et al. Loss of PPAR gamma in immune cells impairs the ability of abscisic acid to improve insulin sensitivity by suppressing monocyte chemoattractant protein-1 expression and macrophage infiltration into white adipose tissue. J Nutr Biochem 2008;19:216–28.
[4] Rosamond W, Flegal K, Furie K, et al. Heart disease and stroke statistics-2008 update: A report from the american heart association statistics committee and stroke statistics subcommittee. Circulation 2008;117:e25–e146.
[5] Bruzzone S, Bodrato N, Usai C, et al. Abscisic acid is an endogenous stimulator of insulin release from human pancreatic islets with cyclic adp ribose as second messenger. J Biol Chem 2008;283:32188–97.
[6] Bers DM. Calcium cycling and signaling in cardiac myocytes. Annu Rev Physiol 2008;70:23–49.
[7] Ban K, Noyan-Ashraf MH, Hoefer J, Bolz SS, Drucker DJ, Husain M. Cardioprotective and vasodilatory actions of glucagon-like peptide 1 receptor are mediated through both glucagon-like peptide 1 receptor-dependent and -independent pathways. Circulation 2008;117:2340–50.
[8] Taussig R, Gilman AG. Mammalian membrane-bound adenylyl cyclases. J Biol Chem 1995;270:1–4.
[9] Berg T, Degerman E, Tasken K. Increased cAMP signaling can ameliorate the hypertensive condition in spontaneously hypertensive rats. J Vasc Res 2009;46: 25–35.
[10] Feldman RD, Gros R. Defective vasodilatory mechanisms in hypertension: A g-protein-coupled receptor perspective. Curr Opin Nephrol Hypertens 2006;15: 135–40.
[11] Murata S, Miniati DN, Kown MH, et al. Elevated cyclic adenosine monophosphate ameliorates ischemia-reperfusion injury in rat cardiac allografts. J Heart Lung Transplant 2003;22:802–9.
[12] Hazell LJ, Baernthaler G, Stocker R. Correlation between intima-to-media ratio, apolipoprotein b-100, myeloperoxidase, and hypochlorite-oxidized proteins in human atherosclerosis. Free Radic Biol Med 2001;31:1254–62.
[13] van Vlijmen BJ, van den Maagdenberg AM, Gijbels MJ, et al. Diet-induced hyperlipoproteinemia and atherosclerosis in apolipoprotein e3-leiden transgenic mice. J Clin Invest 1994;93:1403–10.
[14] Bassaganya-Riera J, Reynolds K, Martino-Catt S, et al. Activation of PPAR gamma and delta by conjugated linoleic acid mediates protection from experimental inflammatory bowel disease. Gastroenterology 2004;127:777–91.
[15] Andersson IJ, Ljungberg A, Svensson L, Gan LM, Oscarsson J, Bergstrom G. Increased atherosclerotic lesion area in ApoE deficient mice overexpressing bovine growth hormone. Atherosclerosis 2006;188:331–40.
[16] Shimokama T, Haraoka S, Watanabe T. Morphological fate and sequelae of human atherosclerosis: Evaluation of immune mechanisms in atherogenesis through immunohistological and ultrastructural analysis. Pathol Int 1995;45:801–14.
[17] Lutgens E, de Muinck ED, Heeneman S, Daemen MJ. Compensatory enlargement and stenosis develop in ApoE(-/-) and ApoE*3-leiden transgenic mice. Arterioscler Thromb Vasc Biol 2001;21:1359–65.
[18] Nakashima Y, Plump AS, Raines EW, Breslow JL, Ross R. ApoE-deficient mice develop lesions of all phases of atherosclerosis throughout the arterial tree. Arterioscler Thromb 1994;14:133–40.
[19] Wittwer J, Hersberger M. The two faces of the 15-lipoxygenase in atherosclerosis. Prostaglandins Leukot Essent Fatty Acids 2007;77:67–77.
[20] Bassaganya-Riera J, Misyak S, Guri AJ, Hontecillas R. PPAR gamma is highly expressed in f4/80(hi) adipose tissue macrophages and dampens adipose-tissue inflammation. Cell Immunol 2009;258:138–46.
[21] D'Angelo G, Lee H, Weiner RI. Camp-dependent protein kinase inhibits the mitogenic action of vascular endothelial growth factor and fibroblast growth factor in capillary endothelial cells by blocking raf activation. J Cell Biochem 1997;67:353–66.
[22] Indolfi C, Avvedimento EV, Di Lorenzo E, et al. Activation of cAMP-pka signaling in vivo inhibits smooth muscle cell proliferation induced by vascular injury. Nat Med 1997;3:775–9.

[23] Morandini R, Ghanem G, Portier-Lemarie A, Robaye B, Renaud A, Boeynaems JM. Action of cAMP on expression and release of adhesion molecules in human endothelial cells. Am J Physiol 1996;270:H807–816.
[24] Moy AB, Bodmer JE, Blackwell K, Shasby S, Shasby DM. Camp protects endothelial barrier function independent of inhibiting mlc20-dependent tension development. Am J Physiol 1998;274:L1024–1029.
[25] Lum H, Jaffe HA, Schulz IT, Masood A, RayChaudhury A, Green RD. Expression of pka inhibitor (pki) gene abolishes cAMP-mediated protection to endothelial barrier dysfunction. Am J Physiol 1999;277:C580–588.
[26] Michell BJ, Chen Z, Tiganis T, et al. Coordinated control of endothelial nitric-oxide synthase phosphorylation by protein kinase c and the cAMP-dependent protein kinase. J Biol Chem 2001;276:17625–8.
[27] Niwano K, Arai M, Tomaru K, Uchiyama T, Ohyama Y, Kurabayashi M. Transcriptional stimulation of the eNOS gene by the stable prostacyclin analogue beraprost is mediated through cAMP-responsive element in vascular endothelial cells: close link between pgi2 signal and no pathways. Circ Res 2003;93:523–30.
[28] Sturla L, Fresia C, Guida L, et al. LANCL2 is necessary for abscisic acid binding and signaling in human granulocytes and in rat insulinoma cells. J Biol Chem 2009.
[29] Pascual G, Fong AL, Ogawa S, et al. A sumoylation-dependent pathway mediates transrepression of inflammatory response genes by PPAR-gamma. Nature 2005;437:759–63.
[30] Magnone M, Bruzzone S, Guida L, et al. Abscisic acid released by human monocytes activates monocytes and vascular smooth muscle cell responses involved in atherogenesis. J Biol Chem 2009.
[31] Karman RJ, Gupta MP, Garcia JG, Hart CM. Exogenous fatty acids modulate the functional and cytotoxic responses of cultured pulmonary artery endothelial cells to oxidant stress. J Lab Clin Med 1997;129:548–56.
[32] Chobanian AV, Alexander RW. Exacerbation of atherosclerosis by hypertension. Potential mechanisms and clinical implications. Arch Intern Med 1996;156: 1952–6.
[33] Knowles JW, Reddick RL, Jennette JC, Shesely EG, Smithies O, Maeda N. Enhanced atherosclerosis and kidney dysfunction in eNOS(-/-)ApoE(-/-) mice are ameliorated by enalapril treatment. J Clin Invest 2000;105:451–8.